ENVIRONMENTAL STUDIES

U.S. fires became larger, more frequent, and more widespread in the 2000s

Virginia Iglesias[1]*, Jennifer K. Balch[1,2], William R. Travis[1,2]

Recent fires have fueled concerns that regional and global warming trends are leading to more extreme burning. We found compelling evidence that average fire events in regions of the United States are up to four times the size, triple the frequency, and more widespread in the 2000s than in the previous two decades. Moreover, the most extreme fires are also larger, more common, and more likely to co-occur with other extreme fires. This documented shift in burning patterns across most of the country aligns with the palpable change in fire dynamics noted by the media, public, and fire-fighting officials.

INTRODUCTION

Fire is an integral component of numerous terrestrial ecosystems (*1*). Recent record-breaking events, unprecedented losses, and escalating suppression costs, however, have raised concerns over a "new normal" of increased fire activity and the onset of an era of megafires (*2*–*4*). In the contiguous United States (CONUS), burning between 2011 and 2016 resulted in ~3.5 billion USD of property and crop damage, ~12.4 billion USD in suppression efforts, and the loss of 162 lives (*5*). Trends toward increasing total burned area over the past several decades have been documented in western CONUS (*6*). Recent large fires in the central grasslands and eastern forests suggest that high-cost, high-loss events may be a continental phenomenon (*7*). Nonetheless, it has yet to be determined whether these changes have been associated with a detectable shift in fire dynamics. We analyzed over 28,000 fires in the Monitoring Trends in Burn Severity (MTBS) dataset (*8*) to (i) test for the presence of shifts in number of fires and area burned; (ii) describe fires before and after shifts in terms of size and frequency; and (iii) quantify how these differences affected the spatial aggregation and probability of co-occurrence of fires. This approach allowed us to rigorously assess the perception that fire behavior has changed across CONUS, recognizing that this is critical to reassessing fire-fighting efforts and delineating priorities for action and strategic resource allocation.

RESULTS

Trends in fire frequency and size shifted in the 2000s

The MTBS program couples the Landsat archive with federal and state fire reports to map burns across the United States. Consistent mapping requires high-quality satellite imagery and reliable fire occurrence information. To satisfy these conditions, MTBS only documents large events, i.e., fires greater than 4 km^2 in western CONUS and larger than 2 km^2 in the east portion of the country (*8*). Between 1984 and 2019, 7841, 2490, and 2759 fires were recorded in the West, Great Plains, and East, affecting ~354,240, 75,760, and 40,410 km^2, respectively. Breakpoint analysis performed with five algorithms with different parameters, penalization criteria (*P* values, Bayesian information criterion, deviance reduction, and penalized likelihood), and distribution assumptions (Gaussian, negative binomial, and distribution free; see the Supplementary Materials for details) reveals that fire patterns were marked by a shift that occurred around the year 2000 (Fig. 1, A to I). Specifically, all five tests identified structural changes in the time series of weekly area burned in the West and Great Plains, and median fire size in the West in 1998–2002, while three tests point to shifts in weekly area burned in the East and fires ignited per week in the West over the same period. Two breakpoints are inferred for fires ignited per week in the Great Plains, the first one in 1999 and the most recent one in 2005. These two breakpoints are supported by three and four tests, respectively. No changes in median fire size in the Great Plains or East were indicated by more than one test (figs. S1 to S5). The consistency of the results suggests that the structural changes in fire detected in the time series are robust to the methodological assumptions of the breakpoint tests.

The power of the series at 1-year periods has increased since 1984 in the three areas. In the West, it was significant in 1984–2018 with the exception of 1989–1993. In the Great Plains and East, it became continuously significant after 2005 (pseudo-$P < 0.05$; Fig. 1, J to L). After ~2000, this yearly recurrence was superimposed on a ~5-year cycle of burning across the country. Fires in the West and Great Plains additionally exhibited more pronounced seasonal oscillations (at 3 to 6 months) starting in ~1994 and ~2005, respectively.

At daily time scales, area burned in the West and Great Plains presents mean Hölder exponents $-1.0 < \overline{h} < -0.5$, indicating that fire dynamics in these regions are strongly antipersistent and stationary. In the East, mean Holder exponents $\overline{h} = -1.06 \pm 0.02$ point to antipersistent but slightly nonstationary behavior (*9*). Comparison of the Hölder exponents estimated before the year 2000 and after 2004 reveals that whereas no statistically significant changes in $\overline{h}$ are observed (pseudo-$P > 0.05$), their SD decreased by a factor of 5 and 2 in the West and Great Plains, respectively, and nearly doubled in the East (fig. S6). These changes in the width of the spectrum can be interpreted as the emergence of more regular patterns of burning in the West and Great Plains and more unpredictable fires in the East (*10*). Together, analyses of the time and frequency domains of fires in CONUS suggest that 2000–2004 were transitional years, and fire dynamics in the West and Great Plains before 2000 and after 2004 are statistically different in terms of extent, number of events, and periodicity. Hereafter, we focus on the comparison of the periods before (1984–1999) and after (2005–2019) this shift in fire activity.

[1]Earth Lab, Cooperative Institute for Research in Environmental Sciences, University of Colorado, Boulder, Boulder, CO 80309, USA. [2]Department of Geography, University of Colorado, Boulder, Boulder, CO 80309, USA.
*Corresponding author. Email: virginia.iglesias@colorado.edu

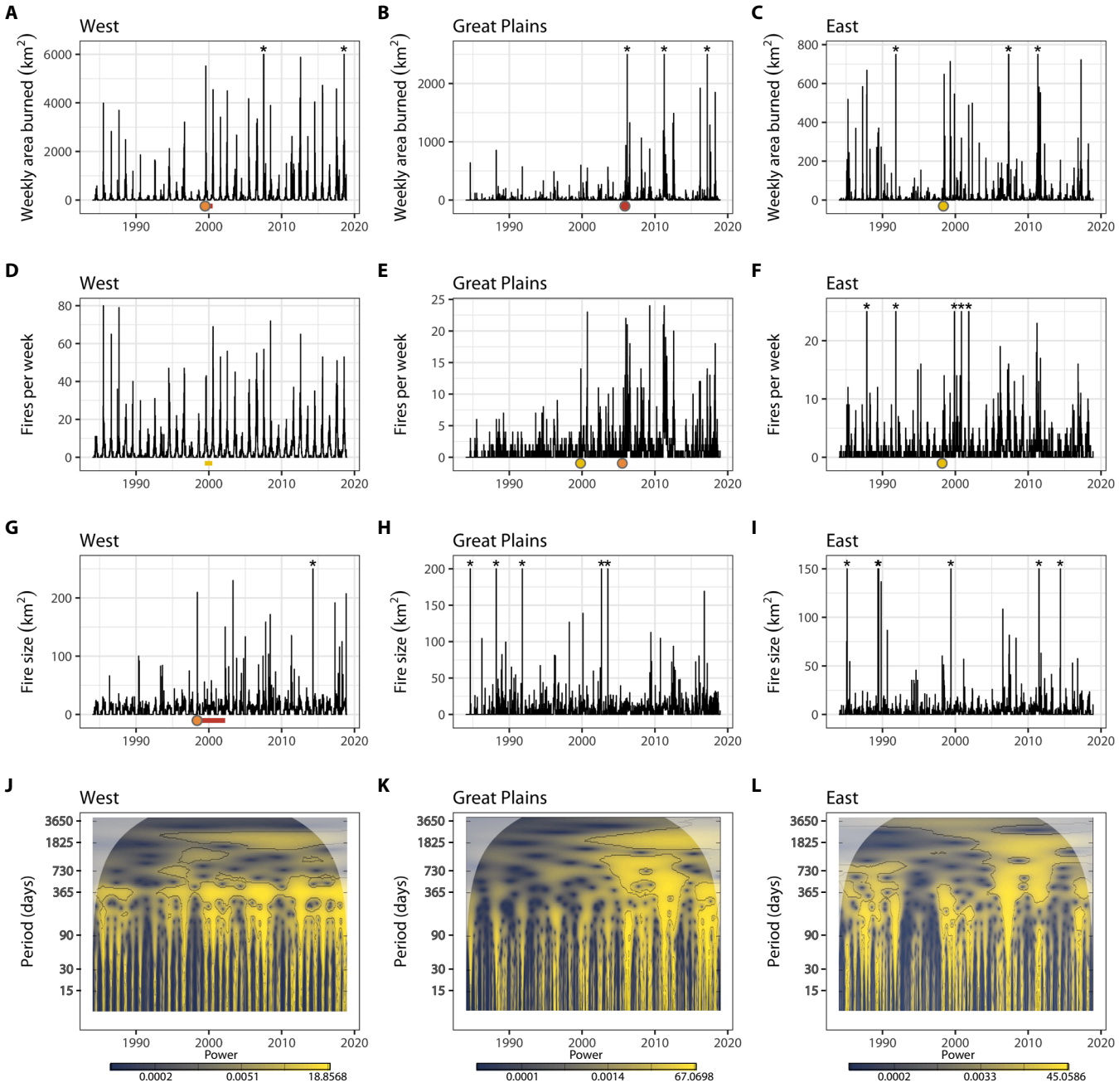

Fig. 1. Temporal trends in fires in the West, Great Plains, and East. (**A** to **C**) Weekly area burned, (**D** to **F**) number of fires per week, and (**G** to **I**) median fire size. Outliers are depicted with asterisk (*). The point location (circles) and intervals (horizontal bars) of breaks in the time series detected by three (yellow), four (orange), and five (red) algorithms are shown at the bottom of each panel (see fig. S4 for details). Absence of circles/horizontal bars indicates that no shifts were detected by at least three statistical tests. Wavelet power spectrum of daily area burned (**J** to **L**). The light shading indicates the cone of influence where edge effects are important, and the black contour lines enclose regions of >95% confidence for departures from a red-noise process.

All regions are affected by more fires

Before 1999, fires affected annual medians of 4019 ± 1204 km^2 in the West, 542 ± 215 km^2 in the Great Plains, and 538 ± 356 km^2 in the East. After 2004, median annual burning rose to 14,249 ± 3164 km^2 and 3354 ± 1314 km^2 in the West and Great Plains, respectively (Fig. 2 and table S1). These increases were associated with more fires in both areas and larger fires in the West. While annual area burned did not change significantly in the East (median = 833 ± 219 km^2), the region experienced an increase in the number of fires per year (Fig. 3 and tables S2 and S3).

The general relationship between number of fires and area burned is approximately linear, i.e., the total area burned per unit of time is directly proportional to the number of fires. This association, however, does not hold when environmental conditions are conducive to a large number of fires. Under these circumstances, the density distribution of weekly area burned becomes multimodal, pointing

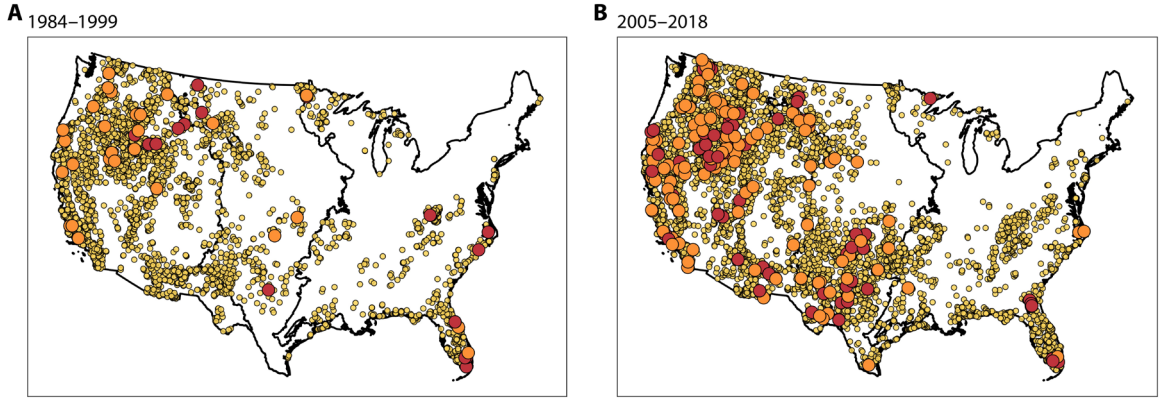

Fig. 2. Spatial distribution of fires. Fires in the West (leftmost region), Great Plains (central region), and East (rightmost region) in (**A**) 1984–1999 and (**B**) 2005–2018. Nonextreme fires are shown with small dots, and extreme fires are represented with larger orange (area burned >99th percentile in 1984–1999) or red bubbles (area burned >99th percentile in 2005–2018).

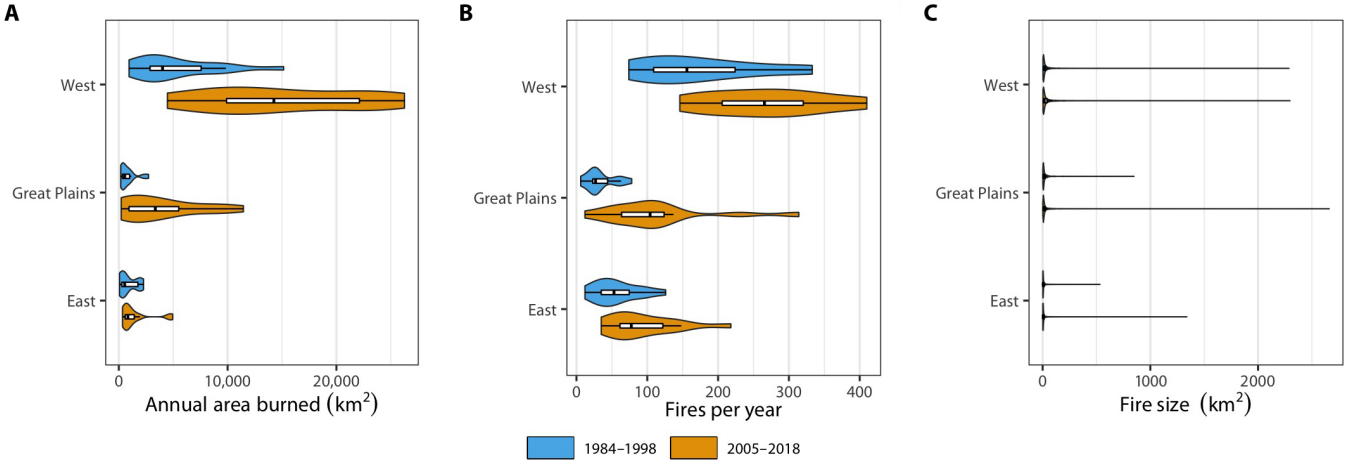

Fig. 3. Fire statistics. Probability distributions of (**A**) annual area burned, (**B**) annual number of fires, and (**C**) fire size, in the West, Great Plains, and East, before (1984–1998) and after (2005–2018) the transition period identified by the breakpoint analysis.

to the existence of a separate class of events: extreme events (Fig. 4). Insights into these unusual, anomalously large events can be gained through exploration of the right tail of the frequency-size distribution. In 1984–1999, 23 fires larger than 285 km^2 (West), 3 fires larger than 223 km^2 (Great Plains), and 3 fires larger than 208 km^2 (East) were in the upper 1% of the distribution. After 2005, 92, 23, and 10 events exceeded those thresholds, and the 99th percentile of the distribution escalated to 694 km^2 in the West (92 events) and 425 km^2 in the Great Plains (17 events). No changes were detected in the East (Figs. 1 to 3 and table S1).

Large fires are temporally concurrent

Fire frequency, whose median before the regime shift was 174 ± 2 events per year in the West, 34 ± 5 events per year in the Great Plains, and 57 ± 8 in the East, rose to 270 ± 21, 113 ± 20, and 94 ± 13, respectively. The inverse of the estimated fire frequency [hereafter expected fire recurrence interval (FRI)] informs on the average time between the ignition of fires in a region. To assess whether fires tend to coincide in time, we compared the expected FRI for each region with the corresponding observed FRI. Observed FRI's were calculated as the time between years when at least one fire was ignited. Expected-to-observed recurrence intervals of fire sizes that were not observed every year were larger than one and increased as a function size, suggesting that large events tend to be concurrent in all regions (Fig. 5).

Recent fires are in closer proximity and more widespread than in the past

Irrespective of fire size, the average distance between fires in 1984–2018 was smaller than if burning had occurred randomly across the country (pseudo-$P < 0.05$). This difference suggests that the spatial aggregation of fires is heterogeneous, with areas affected by several fires coexisting with unburned landscape. The distance between burns across the country decreased after 2004, indicating that, on average, recent fires were in closer proximity than in previous decades (Fig. 6, A to C). Decreased distances between fires do not necessarily imply changes in the spatial distribution of fires, as they could be the product of more fires concentrated in the same clusters as in 1984–1999. To test whether smaller distances had an impact on the spatial arrangement of fires, we accounted for the effects of changes in fire density by generating one random point pattern per year with the same number of points as ignitions were registered

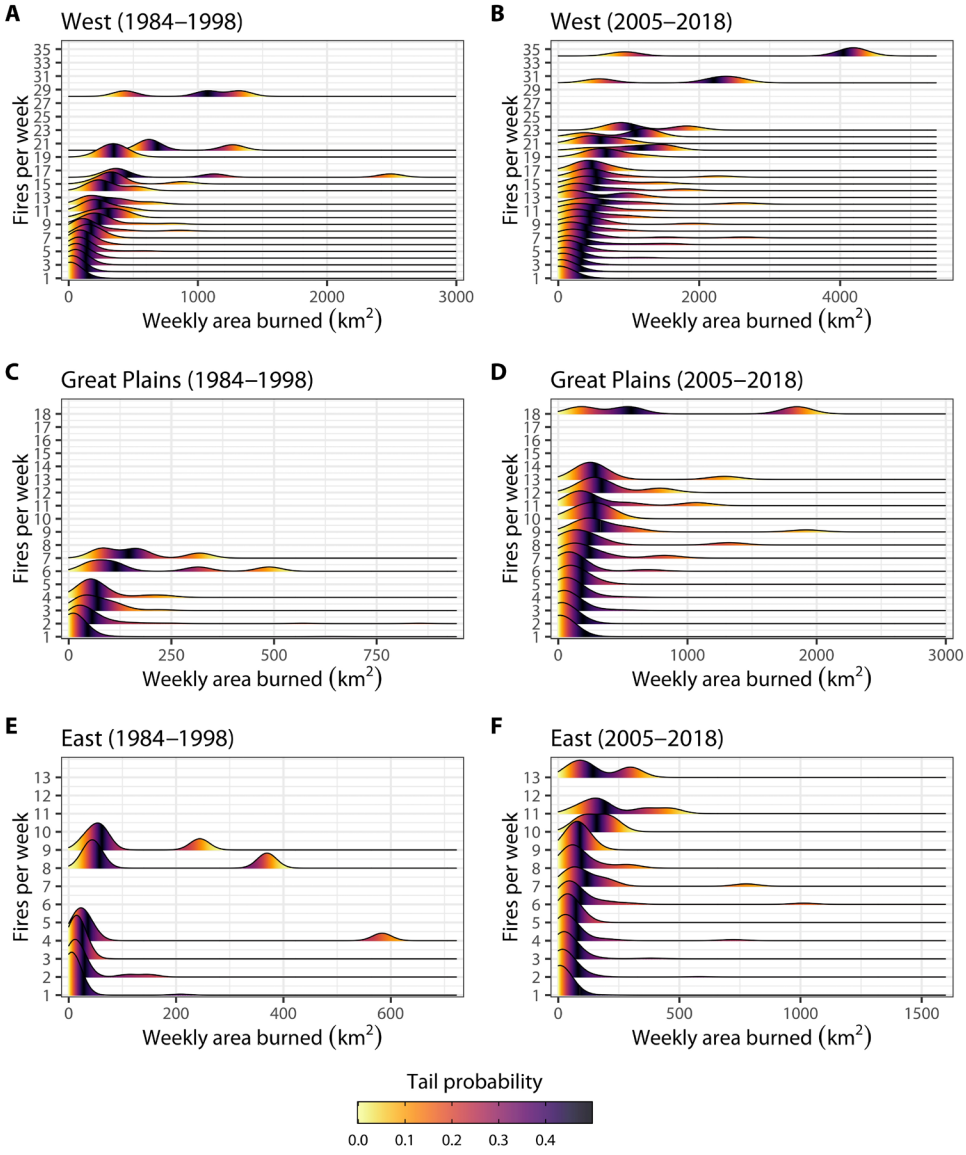

Fig. 4. Changes in the relationship between number of fires and area burned. Kernel-estimated density distribution of weekly area burned as a function of number of fires (bandwidth = 108) in the West (**A** and **B**), Great Plains (**C** and **D**), and East (**E** and **D**), before (1984–1998) and after (2005–2018) the transition period identified by the breakpoint analysis. The color gradient depicts the probability of a value being larger or smaller than the mean given the observed distributions (i.e., tail probability). Note that the limits of the axes are different.

during the same year. Smaller expected-to-observed distance ratios between burns in recent years are consistent with a decrease in clustering and indicate that fires now are more widespread than in 1984–1999 (Fig. 6, D to F).

Testing the robustness of the fire data

Given the dependence of these analyses on robust time series data from the satellite record, we also conducted several tests to confirm that there were no temporal biases associated with different satellites in the Landsat series. This study is based on data obtained from the MTBS program, built on observations from three Landsat satellites. Fire perimeter delineation is guided by state and federal fire history records and performed manually through standardized analysis of Landsat imagery (*8*). The main potential sources of error in this product are therefore associated with fire reporting and changes in Landsat sensors/imagery availability. Should they be temporally biased, errors in MTBS could influence our results. For this reason, we compared annual time series generated from MTBS with Integrated Reporting of Wildland-Fire Information [IRWIN (*11*)], Landsat Burned Area [LBA (*12*)], and Fire Events Delineation [FIRED (*13*); see the Supplementary Materials for details].

Improvements in fire detection capabilities arising from better quality and/or more satellite imagery could be expected to be associated with Landsat 7 and its Enhanced Thematic Mapper Plus sensor (ETM+). Those improvements would have resulted in an overestimation of area burned by MTBS with respect to IRWIN after 1999. No changes in the MTBS-to-IRWIN area burned ratio argue against a temporal bias in the fire time series introduced by the availability of imagery from Landsat 7. Time series of annual area burned, fires per year, and fire size derived from TM and ETM+ scenes are very

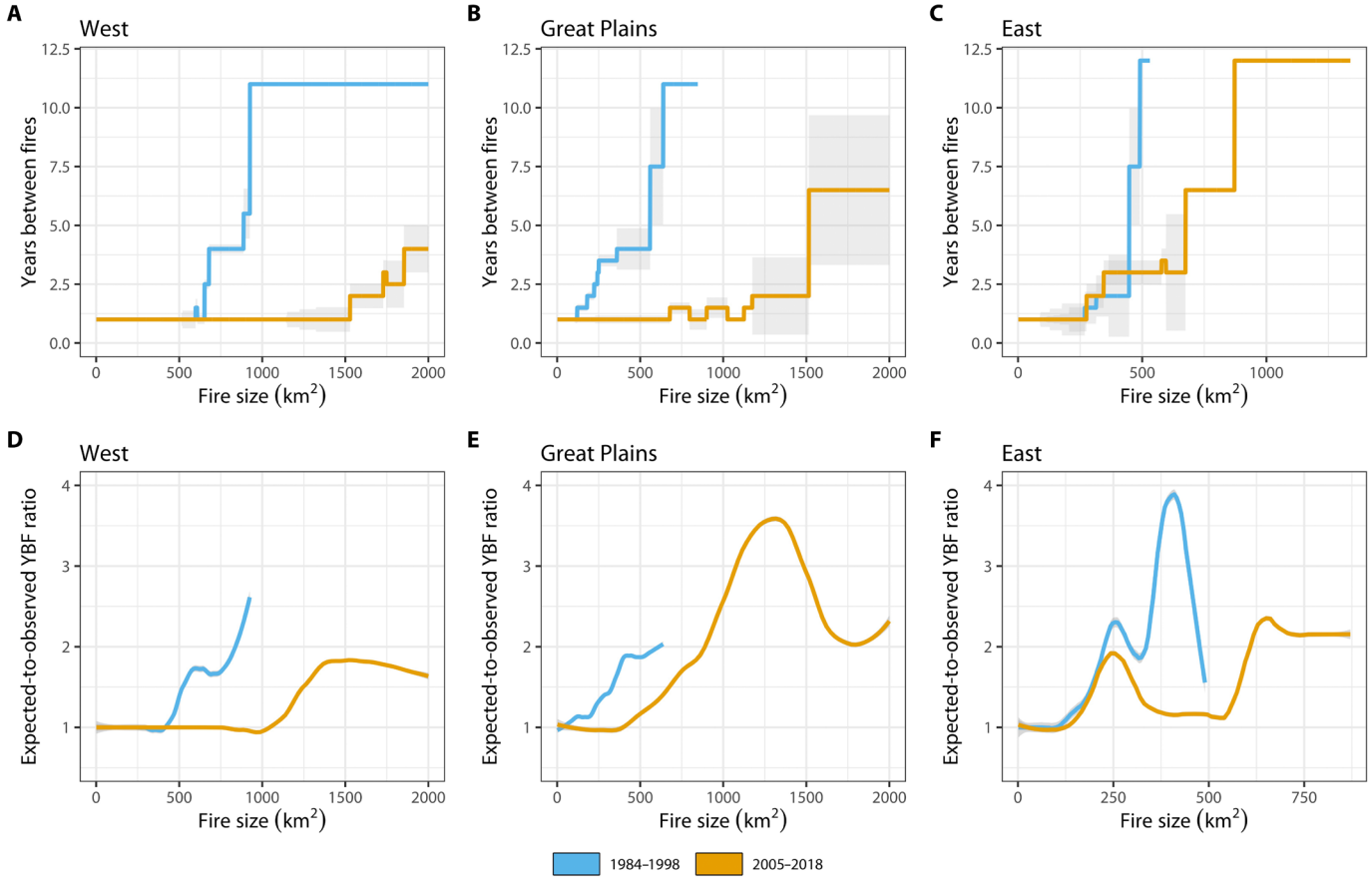

Fig. 5. Co-occurrence of fires in 1984–1999 and 2005–2018. Years between fires as a function of fire size in the (**A**) West, (**B**) Great Plains, and (**C**) East. Expected years between fires (YBFs) relative to fire size in the (**D**) West, (**E**) Great Plains, and (**F**) East. SEs for the estimates are indicated in gray. Note that the limits of the *x* axis are different.

similar (figs. S7 and S8). Further, they show no indication of temporal biases when compared against the FIRED product, derived from the Moderate Resolution Imaging Spectroradiometer (MODIS) Burned Area Product (fig. S9). Last, although absolute values differ among datasets, the relative difference in median annual area in 2005–2018 with respect to 1984–1998 is the same regardless of the data product used in the analysis (pseudo-$P < 0.05$). The same is true for the median and 99th percentile of the annual area burned distribution and for fires ignited per year and fire size (Fig. 7 and tables S1 to S9). These results suggest that, despite omission and commission errors, MTBS time series do not show a temporal bias that could significantly condition our conclusions.

DISCUSSION

Projected changes in climate, fuel, and ignitions suggest that the future of fires does not look like the past (*14*, *15*). Our analyses show that neither does the present. Despite regional differences in effective moisture, vegetation, and land use, the annual number of fires in 2005–2018 nearly doubled in the West and East and quadrupled in the Great Plains with respect to 1984–1999. In addition, individual fires in the West were significantly more extensive than in previous decades. As a result, median annual area burned has quadrupled in the West and grown 620% in the Great Plains. In the East, while the median area affected by fires has remained constant, the top 1% annual area burned has doubled (Figs. 1 to 3 and 7). The reported differences in annual area burned, number of events, and fire size before and after the shift are, in all cases, statistically different from those generated under the null hypothesis that the medians for both periods were equal (pseudo-$P < 0.05$).

More worrisome is the increase in magnitude and frequency of extreme fires in the West and Great Plains. The term "extreme" has multiple meanings in the fire literature (*16*). Here, we use it to refer to the largest fires within a spatiotemporal domain (i.e., 99th percentile of the distribution). Fires that are extreme in terms of their physical properties, be it size, intensity, or spread rate, are not necessarily the most devastating ones, as impact also depends on exposure and vulnerability of social-environmental systems (*17*). However, it is important to understand the dynamics of large fires because of the heavy-tailed nature of the fire size-frequency distribution (Figs. 3 and 4) (*18*). This type of distribution has three main consequences of social and ecological relevance: (i) Estimates of the central tendency are a less adequate representation of expected fire size than for normally distributed populations, (ii) the probability of record-breaking fires is nonnegligible, and (iii) extreme fires account for a disproportionately large fraction of total area burned and fire emissions, substantially affecting air pollution, public health, and climate (*19*–*21*).

As predicted for extreme events in theoretical physical systems (*22*), both pre- and postshift extreme fires tend to be concurrent. The causes of extreme flammability cannot be generalized, as the

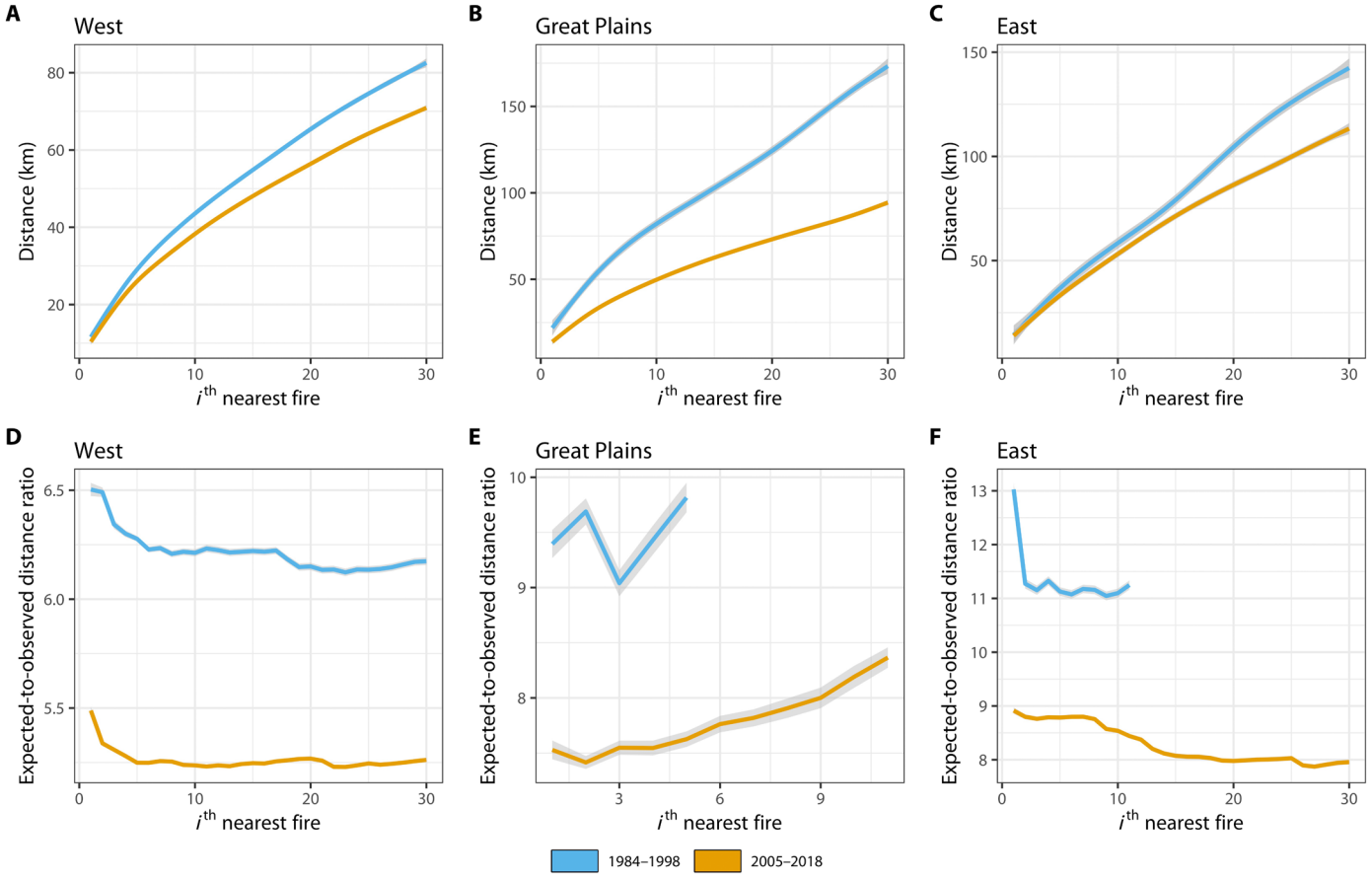

Fig. 6. Spatial aggregation of fires in 1984–1999 and 2005–2018. Locally weighted scatterplot smoothing of median distances between a fire and the *i*th nearest fire in the (**A**) West, (**B**) Great Plains, and (**C**) East. Theoretical distance between fires generated by a random independent process relative to the observed distance between a fire and the *i*th nearest fire in the (**D**) West, (**E**) Great Plains, and (**F**) East. Ninety-five percent of confidence intervals for the estimates are shown in gray. Note that the limits of the axes are different.

relative importance of fire drivers, including climate, topography, vegetation, and weather, changes when critical thresholds are reached (*23*). It is clear, nonetheless, that some years feature only average fires, but when conditions are conducive for extreme fire activity, more than one extreme event occurs (Fig. 5). An example of this phenomenon comes from the southern Great plains. During the second week of April 2011, a low-level thermal ridge associated with temperatures of ~37°C, 5 to 15% relative humidity, and wind gusts of up to 65 km hour^{-1} created persistent critical fire weather across the area. Four extreme fires in Texas resulted in 96% of the 3000 km^2 burned during this perfect storm (Fig. 4D) and caused more damage than in any previous year of Texas fires (*24*). These nonlinear dynamics suggest that extreme fires are an emergent property of socioenvironmental systems, and anticipating their future occurrence may be challenging (*17*, *25*).

Several studies have documented a strong correlation between fuel aridity during the fire season and area burned in the western United States [e.g., (*26*, *27*)]. Vapor pressure deficit (the depression of the water content of the atmosphere below the saturation point) in this region has increased notably over the past few decades (*28*). The resulting aridification, which showed a step-like increase in 2000–2003, has doubled the extent of fire prone ecosystems in the West (*29*). Although natural variability played a role, up to two-thirds of this increase in aridity has been attributed to anthropogenic warming (*30*, *31*).

Anthropogenic effects are likely to have influenced fire patterns across the country not only indirectly through regional aridification [shown in the West (*26*), yet to be tested in the Great Plains and East] but also in a direct manner. During the last 21 years, for example, human ignitions caused 84% of all fires in CONUS, representing approximately 40,000 fires per year (*32*). Concurrent ignition and dry fuels are prerequisites for burning. By introducing ignitions into dry landscapes, humans have tripled the length of the fire season and expanded the size of fire-prone areas. These ignitions are notoriously important in regions with sufficient dry fuel to support fires but where lightning concurrent with dry fuel is rare, such as large portions of the Great Plains and eastern United States (*33*).

Interactions between climate, topography, and anthropogenic impact associated with recreation, ecosystem management, increased use of prescribed fire, and development, affect fire behavior in complex ways. Variability in the nature and strength of these interactions is reflected in the heterogeneous spatial distribution of large fires across CONUS (Fig. 2). Very few events in the Pacific Northwest and in the central and northeastern portions of the country contrast with clusters of fires in the remaining areas. The geographical arrangement of burns within these fire-prone ecosystems has changed,

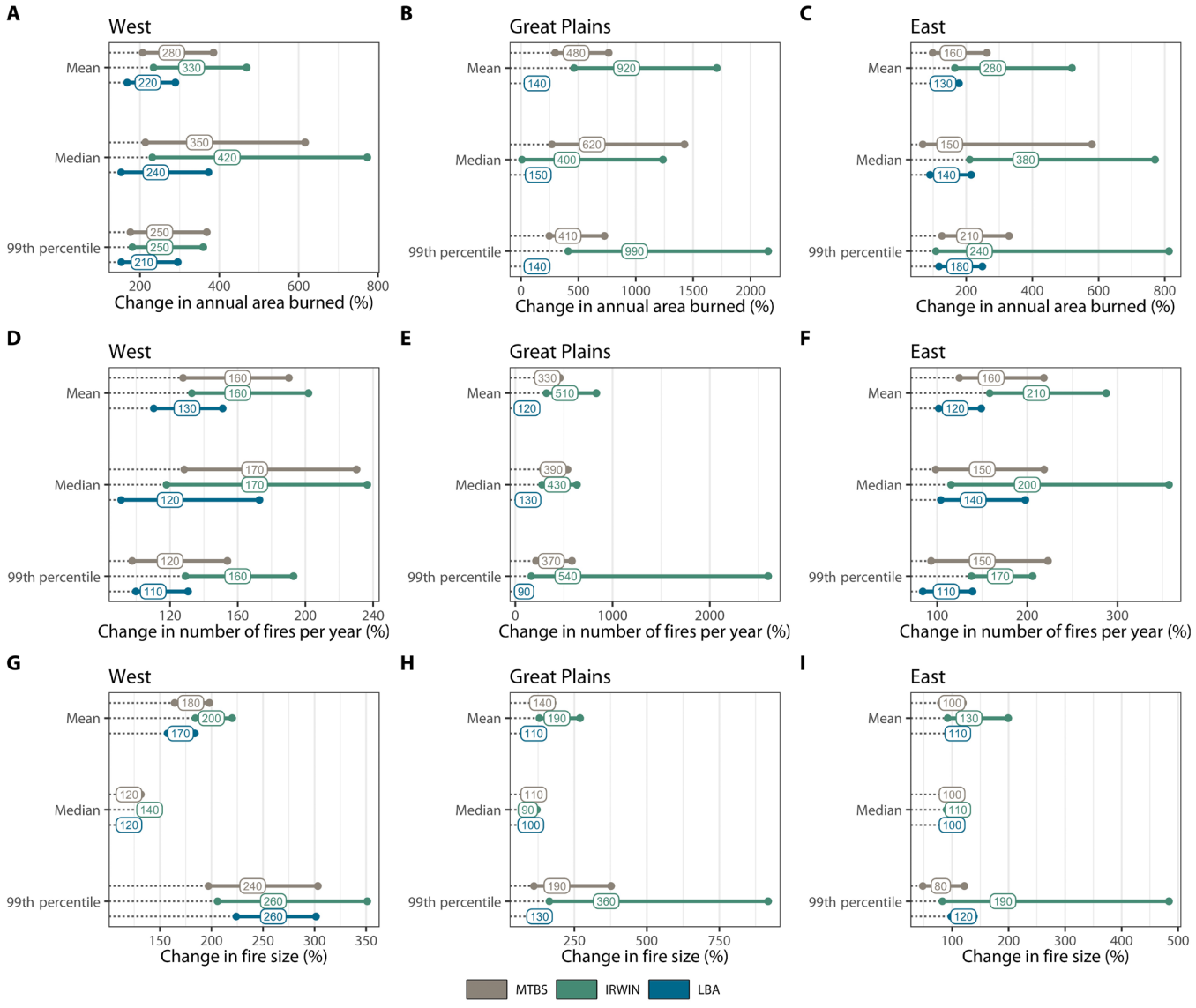

Fig. 7. Summary statistics in 2005–2018 relative to 1984–1998 (%) as estimated from MTBS, IRWIN, and LBA. Changes in area burned in the (**A**) West, (**B**) Great Plains, and (**C**) East. Changes in the number of fires per year in the (**D**) West, (**E**) Great Plains, and (**F**) East. Changes in fire size in the (**G**) West, (**H**) Great Plains, and (**I**) East.

as fires today occur in closer proximity than in the past. For example, we show that the mean distance between a fire ignition point and the 10th nearest fire in 1984–1999 was 120, 160, and 115% larger than in 2005–2018 in the West, Great Plains, and East (Fig. 6, A to C). Considering that the size of the mean and extreme fire has increased (Fig. 3 and table S1), the decrease in mean distance between fire perimeters is likely to be larger than these results would suggest.

Smaller distances can be expected from an increase in the number of events observed across the country. When accounting for changes in fire density, we found that burns are not randomly distributed in space but rather tend to be grouped in "fire hot spots" within flammable ecosystems. In recent years, fires have become less clustered than before, possibly reflecting increases in the size of these hot spots associated with higher probability of ignition and, at least in the West, a growing fire-prone landscape largely resulting from climate change (Fig. 6, D to F).

In addition to changes in size, frequency, and spatial distribution of fires that we report, an overall eightfold increase in annual area burned at high severity has been documented in 1985–2017 (*34*). It has yet to be assessed whether other properties of the fire regime, such as fire spread rates and intensity, remain stationary. Potential impacts of the shift in fire patterns are already manifest across ecoregions. Young conifer stands in subalpine and alpine forests, for instance, are reburning before developing fire resistance, which hinders tree regeneration and possibly delays aboveground carbon recovery for >150 years (*35*). Changing burning patterns, in cases mediated by invasive species (*36*), have also been registered at lower elevations where fires once played a vegetation-maintenance role (*37*). As a result, certain fires now threaten the persistence of species they once favored. Further, fire has emerged as one of the main drivers of the tree mortality that the western United States is facing (*38*).

Fire impacts propagate through ecosystem processes, potentially altering land surface dynamics. This is evident in burned forests of the intermountain West, where solar forcing on snow has exhibited a fourfold increase in the 2000s and led to earlier snowmelt and lower streamflow during the summer (*39*). Cascading impacts could ultimately compromise ecosystem services including water supply, recreation, tourism, and air quality for the 30 million Americans and >900,000 residential properties exposed to significant fire hazard (*40*, *41*).

The record-breaking fire season in 2020 in the West speaks to continuation of the altered fire patterns that we documented. Even if our data do not point to a statistically significant increase in annual area burned in the East, it is possible that changes in fire dynamics may also be underway, signaled by (i) increased fire frequency, (ii) potential nonstationarity of the daily area burned time series, (iii) changes in the tail of the fire size-frequency distribution reflecting devastating events such as the Great Smokies fire complex in 2016, and (iv) in the spatial rearrangement of ignition points. As housing developments continue to expand into flammable vegetation (*41*), fires will increasingly jeopardize lives and properties, and suppression costs, which already represent >50% of U.S. Forest Service budget, will rise (*42*). High-cost, high-loss events like the 2018 Camp Fire in California, which resulted in 85 fatalities and damage estimated at 16.5 billion USD, exemplify this rising risk and indicate that fire suppression capabilities may have already been exceeded. Extreme, co-occurring fires will further challenge fire-fighting efforts, emergency response, and resource allocation (*43*), disproportionately affecting vulnerable communities (*44*) and groups that have not been as exposed to large fires in the past. The apparent shift to more extreme burning in the United States has evoked a searching discussion about our relationship with fires, which have "joined the forlorn polar bear as an emblem of a climate crisis" (*45*). Adaptation to these emerging regimes requires that we rethink our priorities for action, especially given large discrepancies in ecological and social vulnerability.

MATERIALS AND METHODS

We acquired fire data for the conterminous United States released on 27 September 2020 by the MTBS program (www.mtbs.gov). MTBS products are generated through standardized analysis of Landsat imagery and the best available state and federal fire history records (*8*). The resulting datasets have consistent coverage of public and private lands and include fires greater than 4 km^2 in the western United States and greater than 2 km^2 in the east from 1984 to 2018.

Recent studies show pronounced differences in fire characteristics across the United States, with larger, infrequent or moderately frequent, mostly lightning-ignited fires in the west of the country, and smaller, frequent fires, mainly started by humans in the east (*33*). To avoid differences in fire size and frequency between ecosystems from dominating the signal, we followed (*12*) and divided CONUS into three broad areas. The western sector ("West") comprises ecoregions 6, 7, and 10 to 12, the "Great Plains" overlaps with ecoregion 13, and the eastern sector ("East") groups ecoregions 5, 8, 9, and 15, as defined by the Commission for Environmental Cooperation (*46*). It is noteworthy that fire behavior within these mapping zones is heterogeneous, and analyses at this scale smooth out important ecosystem-specific variability.

We aggregated the fire data at daily time steps and calculated the number of fire events and total area burned in the West and in the East for every day between 1 February 1984 and 31 December 2018. MTBS reports total area burned per event but does not provide information about the daily evolution of each fire. For this reason, "number of fires" refers to the sum of fires ignited on any given day, and "area burned" corresponds to the final size of each fire scar. In both cases, the date assigned to the fire is that of the day of ignition. The resulting time series were used to (i) test for the presence of shifts in number of fires and area burned, (ii) describe fires before and after the shift in terms of size and frequency, and (iii) quantify how these differences affected the spatial aggregation and probability of co-occurrence of fires.

Statistical analysis

Detection of temporal changes in fire

We took a twofold approach to identifying and testing for the presence of changes in temporal patterns of fire occurrence and extent. First, we used breakpoint analysis to estimate the optimal number and location of shifts in weekly area burned, fires ignited per week, and median fire size in the West, Great Plains, and the East. In all cases, data at weekly time scales were used in the analyses to reduce the noise of the time series of daily burning. Given that breakpoint estimation is sensitive to the methodological assumptions of the analysis, we used five different algorithms to identify the optimal number of breakpoints and evaluate them against the null hypothesis of no change in the mean (i.e., optimal number of breakpoints = 0). We then compared the output of the tests to identify the location of the breakpoints (see the Supplementary Materials and figs. S1 to S5 for details).

Second, we decomposed the time series of daily area burned into the frequency space to determine dominant modes of variability and their temporal dynamics. Specifically, we computed the power spectrum of each series by applying the continuous Morlet wavelet transform at a daily resolution (*47*). Spectral estimates were tested against the null hypothesis that they were indistinguishable from red noise as defined by the autocorrelation of the time series at lag one (1000 simulations; pseudo-$P < 0.05$). Last, we followed Scafetta *et al.* (*10*) to estimate the local Hölder exponent of the singularities of each time series and assess changes in the stationarity and/or persistence of daily area burned in the West, Great Pains, and East (see Supplementary Materials and fig. S6 for details).

Differences in area burned, number of fires, and fire size before and after the shift

We calculated changes in area burned as the difference in weekly area burned corresponding to the median and 99th percentile of the distribution before and after the shifts. We estimated the probability of observing such differences under the null hypothesis that the statistics for both periods were equal. The distribution of the null hypothesis was generated by randomly shuffling weekly area burned values (5000 permutations) and calculating the difference in the simulated medians and 99th percentiles before and after the shift. The same approach was followed to evaluate changes in the number of fires ignited per week and fire size. In all cases, SEs were estimated on the basis of 5000 bootstrap replicates.

Assessment of co-occurrence and spatial arrangement of fires

To evaluate changes in the probability of correlated fires (i.e., two or more fires being ignited in the same region during the same year) of sizes 2 to 2000 km^2, we calculated the expected (Eq. (1) and observed (Eq. 2) FRIs for the West and the Great Plains, before and after the shift. In the East, we assessed the co-occurrence of fires up to

1000 km^2 because very few fires larger than this size have been observed in the area

$$FRIe_{(P,R)} = l_{(P)} * fires_{(P,R)}^{-1} \quad (1)$$

where $FRIe_{(P,R)}$ is the expected FRI for periods P = (1984–1999 and 2005–2018) and regions R = (West, Great Plains, and East), $l_{(P)}$ is length of the period P, in years, and $fires_{(P,R)}$ is the total number of fires during the period P in region R

$$FRIo_{(P,R)} = mean(time_{(P,R)}) \quad (2)$$

where $FRIo_{(P,R)}$ is the observed FRI for periods P = (1984–1999 and 2005–2018) and regions R = (West, Great Plains, and East), and $time_{(P,R)}$ is the time between years with at least one fire in region R during period P.

$FRIe_{(P,R)}$ is the inverse of fire frequency and, therefore, a function of all the fires registered in each area before and after the shift. Conversely, $FRIo_{(P,R)}$ is based on the binary classification of time into years without fires and years when burning occurred, irrespectively of the number of events. For this reason, observed FRIs larger than expected FRIs are indicative of correlated fires.

Last, we assessed the spatial aggregation of fires by computing the mean distance between the location of the ignition point of each fire and the first, second, …, 50th nearest ignition point for every year in the series. Differences in these series in the pre- and postshift periods inform on changes in the proximity of fires. Next, we compared these distances to those resulting from point patterns generated by processes that assumed that (i) all locations had equal probability of burning and (ii) the locations of fires were independent of each other. This comparison allowed us to evaluate whether the observed fires were more or less dispersed than a random independent point pattern.

However, differences in the distance between ignition points before and after the shift do not necessarily imply variations in the spatial clustering of fires, as they may result only from changes in the number of fires on the landscape (i.e., more fires in the same area imply smaller distances). For this reason, we accounted for the effects of fire density by generating one random point pattern per year with the same number of points as ignitions were registered during the same year. In total, we produced 34 random processes, which allowed us to calculate the ratio between random and observed distances between ignition points. We interpret contrasts in these ratios before and after the shifts as evidence of temporal changes in clustering.

Testing the robustness of the fire data

Our results depend on robust time series data from the satellite record. For this reason, we compared the time series of annual area burned, fires ignited per year, and fire size to those derived from IRWIN (*11*), LBA (*12*), and MODIS FIRED algorithm (*13*). We then evaluated whether there were differences among products in the mean, median, and 99th percentile of the distributions before and after the shift. This allowed us to assess the potential presence of a temporal bias in the MTBS time series that could influence our results. All analyses and figures were performed with R programming language version 3.6.2 (*48*), packages boot 1.3-23 (*49*), breakpoint 1.2 (*50*), changepoint 2.2.2 (*51*), ggridges 0.5.2 (*52*), maptools 1.0-2 (*53*), raster 3.3-13 (*54*), rgdal 1.15-17 (*55*), rgeos 0.5-5 (*56*), sp. 1.4-4 (*57*), spatstat 1-42 (*58*), tidyverse 1.3.0 (*59*), tree 1.4-40 (*60*), viridis 0.5.1 (*61*), WaveletComp 1.1 (*62*), wmtsa 2.1 (*63*), zoo 1.8-8 (*64*), and corresponding dependencies.

SUPPLEMENTARY MATERIALS

Supplementary material for this article is available at https://science.org/doi/10.1126/sciadv.abc0020

REFERENCES AND NOTES

1. A. C. Scott, I. J. Glasspool, The diversification of Paleozoic fire systems and fluctuations in atmospheric oxygen concentration. *Proc. Natl. Acad. Sci. U.S.A.* **103**, 10861–10865 (2006).
2. J. Williams, L. Hamilton, R. Mann, M. Rousanville, H. Leonard, O. Daniels, D. Bunnell, S. Mann, *The Mega-Fire Phenomenon: Toward a More Effective Management Model* (The Brookings Institution, Center for Public Policy Education, 2005).
3. S. J. Pyne, in *Proceedings of the 4th International Wildland Fire Conference*, Seville, Spain, 13 to 17 May 2007 (2007), pp. 1–7.
4. P. Attiwill, D. Binkley, Exploring the mega-fire reality: A 'forest ecology and management' conference. *For. Ecol. Manage.* **294**, 1–3 (2013).
5. CEMHS, *Spatial Hazard Events and Losses Database for the United States* (Center for Emergency Management and Homeland Security, Arizona State University, 2019); https://sheldus.asu.edu/SHELDUS/.
6. P. E. Dennison, S. C. Brewer, J. D. Arnold, M. A. Moritz, Large wildfire trends in the western United States, 1984-2011. *Geophys. Res. Lett.* **41**, 2928–2933 (2014).
7. L. Shore, "2016–2018 southern plains wildfire assessment" (Oklahoma Panhandle Research and Extension Center, 2019), p. 26.
8. J. Eidenshink, B. Schwind, K. Brewer, Z.-L. Zhu, B. Quayle, S. Howard, A project for monitoring trends in burn severity. *Fire Ecol.* **3**, 3–21 (2007).
9. B. Mandelbrot, *The Fractal Geometry of Nature* (Freeman, 1983).
10. N. Scafetta, L. Griffin, B. J. West, Hölder exponent spectra for human gait. *Phys. A Stat. Mech. Appl.* **328**, 561–583 (2003).
11. IRWIN, *Integrated Reporting of Wildland-Fire Information (IRWIN)*; www.forestsandrangelands.gov/WFIT/applications/IRWIN/index.shtml.
12. T. J. Hawbaker, M. K. Vanderhoof, G. L. Schmidt, Y.-J. Beal, J. J. Picotte, J. D. Takacs, J. T. Falgout, J. L. Dwyer, The Landsat Burned Area algorithm and products for the conterminous United States. *Remote Sens. Environ.* **244**, 111801 (2020).
13. J. K. Balch, L. A. S. Denis, A. L. Mahood, N. P. Mietkiewicz, T. M. Williams, J. McGlinchy, M. C. Cook, FIRED (Fire Events Delineation): An open, flexible algorithm and database of US fire events derived from the MODIS Burned Area Product (2001–2019). *Remote Sens. (Basel)* **12**, 3498 (2020).
14. M. B. Joseph, M. W. Rossi, N. P. Mietkiewicz, A. L. Mahood, M. E. Cattau, L. A. S. Denis, R. C. Nagy, V. Iglesias, J. T. Abatzoglou, J. K. Balch, Spatiotemporal prediction of wildfire size extremes with Bayesian finite sample maxima. *Ecol. Appl.* **29**, e01898 (2019).
15. A. L. Westerling, M. G. Turner, E. A. H. Smithwick, W. H. Romme, M. G. Ryan, Continued warming could transform Greater Yellowstone fire regimes by mid-21st century. *Proc. Natl. Acad. Sci. U.S.A.* **108**, 13165–13170 (2011).
16. F. Tedim, V. Leone, M. Amraoui, C. Bouillon, M. Coughlan, G. Delogu, P. Fernandes, C. Ferreira, S. McCaffrey, T. McGee, J. Parente, D. Paton, M. Pereira, L. Ribeiro, D. Viegas, G. Xanthopoulos, Defining extreme wildfire events: Difficulties, challenges, and impacts. *Fire* **1**, 9 (2018).
17. J. K. Balch, V. Iglesias, A. Braswell, M. W. Rossi, M. B. Joseph, A. L. Mahood, T. Shrum, C. White, V. Scholl, B. McGuire, C. Karban, M. Buckland, W. Travis, Social-environmental extremes: Rethinking extraordinary events as outcomes of interacting biophysical and social systems. *Earth's Future* **8**, e2019EF001319 (2020).
18. B. D. Malamud, G. Morein, D. L. Turcotte, Forest fires: An example of self-organized critical behavior. *Science* **281**, 1840–1842 (1998).
19. D. V. Spracklen, L. Garcia-Carreras, The impact of Amazonian deforestation on Amazon basin rainfall. *Geophys. Res. Lett.* **42**, 9546–9552 (2015).
20. X. Yue, L. J. Mickley, J. A. Logan, Projection of wildfire activity in southern California in the mid-twenty-first century. *Climate Dynam.* **43**, 1973–1991 (2014).
21. J. C. Liu, L. J. Mickley, M. P. Sulprizio, F. Dominici, X. Yue, K. Ebisu, G. B. Anderson, R. F. A. Khan, M. A. Bravo, M. L. Bell, Particulate air pollution from wildfires in the Western US under climate change. *Clim. Change* **138**, 655–666 (2016).
22. M. I. Bogachev, J. F. Eichner, A. Bunde, Effect of nonlinear correlations on the statistics of return intervals in multifractal data sets. *Phys. Rev. Lett.* **99**, 240601 (2007).
23. D. McKenzie, M. C. Kennedy, Power laws reveal phase transitions in landscape controls of fire regimes. *Nat. Commun.* **3**, 726 (2012).
24. Texas A&M Forest Service, "2011 Texas wildfires: Common denominators of home destruction" (A&M Forest Service, 2011), p. 50.
25. A. S. Sharma, D. N. Baker, A. Bhattacharyya, A. Bunde, V. P. Dimri, H. K. Gupta, V. K. Gupta, S. Lovejoy, I. G. Main, D. Schertzer, H. von Storch, N. W. Watkins, in *Geophysical*

Monograph Series, A. S. Sharma, A. Bunde, V. P. Dimri, D. N. Baker, Eds. (American Geophysical Union, 2012), vol. 196, pp. 1–16; https://agupubs.onlinelibrary.wiley.com/doi/10.1029/2012GM001233.
26. J. T. Abatzoglou, C. A. Kolden, Relationships between climate and macroscale area burned in the western United States. *Int. J. Wildland Fire* **22**, 1003 (2013).
27. J. S. Littell, D. McKenzie, D. L. Peterson, A. L. Westerling, Climate and wildfire area burned in western U.S. ecoprovinces, 1916–2003. *Ecol. Appl.* **19**, 1003–1021 (2009).
28. R. Seager, D. Neelin, I. Simpson, H. Liu, N. Henderson, T. Shaw, Y. Kushnir, M. Ting, B. Cook, Dynamical and thermodynamical causes of large-scale changes in the hydrological cycle over North America in response to global warming. *J. Climate* **27**, 7921–7948 (2014).
29. J. T. Abatzoglou, A. P. Williams, Impact of anthropogenic climate change on wildfire across western US forests. *Proc. Natl. Acad. Sci. U.S.A.* **113**, 11770–11775 (2016).
30. A. P. Williams, E. R. Cook, J. E. Smerdon, B. I. Cook, J. T. Abatzoglou, K. Bolles, S. H. Baek, A. M. Badger, B. Livneh, Large contribution from anthropogenic warming to an emerging North American megadrought. *Science* **368**, 314–318 (2020).
31. Y. Zhuang, R. Fu, B. D. Santer, R. E. Dickinson, A. Hall, Quantifying contributions of natural variability and anthropogenic forcings on increased fire weather risk over the western United States. *Proc. Natl. Acad. Sci. U.S.A.* **118**, e2111875118 (2021).
32. J. K. Balch, B. A. Bradley, J. T. Abatzoglou, R. C. Nagy, E. J. Fusco, A. L. Mahood, Human-started wildfires expand the fire niche across the United States. *Proc. Natl. Acad. Sci. U.S.A.* **114**, 2946–2951 (2017).
33. R. C. Nagy, E. Fusco, B. Bradley, J. T. Abatzoglou, J. K. Balch, Human-related ignitions increase the number of large wildfires across U.S. ecoregions. *Fire* **1**, 4 (2018).
34. S. A. Parks, J. T. Abatzoglou, Warmer and drier fire seasons contribute to increases in area burned at high severity in western US forests from 1985 to 2017. *Geophys. Res. Lett.* **47**, e2020GL089858 (2020).
35. M. G. Turner, K. H. Braziunas, W. D. Hansen, B. J. Harvey, Short-interval severe fire erodes the resilience of subalpine lodgepole pine forests. *Proc. Natl. Acad. Sci. U.S.A.* **116**, 11319–11328 (2019).
36. E. J. Fusco, J. T. Finn, J. K. Balch, R. C. Nagy, B. A. Bradley, Invasive grasses increase fire occurrence and frequency across US ecoregions. *Proc. Natl. Acad. Sci. U.S.A.* **116**, 23594–23599 (2019).
37. J. Williams, A. Hyde, The mega-fire phenomenon: Observations from a coarse-scale assessment with implications for foresters, land managers, and policy-makers. (Society of American Foresters, Orlando, FI, 2009).
38. H. Stanke, A. O. Finley, G. M. Domke, A. S. Weed, D. W. MacFarlane, Over half of western United States' most abundant tree species in decline. *Nat. Commun.* **12**, 451 (2021).
39. K. E. Gleason, J. R. McConnell, M. M. Arienzo, N. Chellman, W. M. Calvin, Four-fold increase in solar forcing on snow in western U.S. burned forests since 1999. *Nat. Commun.* **10**, 2026 (2019).
40. H. Botts, S. McCabe, B. Stueck, L. Suhr, "Wildfire hazard risk" (Corelogic, 2015).
41. V. Iglesias, A. Brasswell, M. Joseph, C. McShane, M. Rossi, M. Cattau, M. Koontz, J. McGlinchy, R. Nagy, J. Balch, W. Travis, Risky development: Increasing exposure to natural hazards in the United States. *Earth's Future* **9**, e2020EF001795 (2021).
42. T. Schoennagel, J. K. Balch, H. Brenkert-Smith, P. E. Dennison, B. J. Harvey, M. A. Krawchuk, N. Mietkiewicz, P. Morgan, M. A. Moritz, R. Rasker, M. G. Turner, C. Whitlock, Adapt to more wildfire in western North American forests as climate changes. *Proc. Natl. Acad. Sci. U.S.A.* **114**, 4582–4590 (2017).
43. R. Gorte, "The rising cost of wildfire protection" (Headwaters Economics, 2013), p. 16.
44. I. P. Davies, R. D. Haugo, J. C. Robertson, P. S. Levin, The unequal vulnerability of communities of color to wildfire. *PLOS ONE* **13**, e0205825 (2018).
45. S. J. Pyne, From pleistocene to pyrocene: Fire replaces ice. *Earth's Future* **8**, e2020EF001722 (Commission for Environmental Cooperation, 2020).
46. Commission for Environmental Cooperation, *Ecological Regions of North America: Toward a Common Perspective* (2006).
47. C. Torrence, G. P. Compo, A practical guide to wavelet analysis. *Bull. Am. Meteorol. Soc.* **79**, 61–78 (1998).
48. R Core Team, *R: A Language and Environment for Statistical Computing* (The R Foundation, 2019); www.R-project.org/.
49. A. Canty, B. Ripley, *boot: Bootstrap R (S-Plus) Functions* (R package v. 1.3-28, 2019).
50. W. Priyadarshana, G. Sofronov, *Breakpoint: An R Package for Multiple Break-Point Detection via the Cross-Entropy Method* (R package v. 1.2, 2019); https://CRAN.R-project.org/package=breakpoint.
51. R. Killick, I. A. Eckley, changepoint: An R package for changepoint analysis. *J. Stat. Softw.* **58**, 1–19 (2014).
52. C. Wilke, *ggridges: Ridgeline plots in "ggplot2"* (R package v. 0.5.2, 2020).
53. R. Bivand, N. Lewin-Koh, *maptools: Tools for Handling Spatial Objects* (R package v. 1.0-2, 2020); https://CRAN.R-project.org/package=maptools.
54. R. Hijmans, *raster: Geographic Data Analysis and Modeling* (R package v., 2022); https://CRAN.R-project.org/package=raster.
55. R. Bivand, T. Keith, B. Rowlingson, *rgdal: Bindings for the "Geospatial" Data Abstraction Library* (R package v. 1.5-17, 2020); https://CRAN.R-project.org/package=rgdal.
56. R. Bivand, C. Rundel, *rgeos: Interface to Geometry Engine - Open Source ('GEOS')* (R package v. 0.5-5, 2020); https://CRAN.R-project.org/package=rgeos.
57. R. Bivand, E. Pebesma, V. Gomez-Rubio, *Applied Spatial Data Analysis with R* (Springer, 2013); https://asdar-book.org/.
58. A. Baddeley, E. Rubak, R. Turner, *Spatial Point Patterns: Methodology and Applications with R* (Chapman and Hall/CRC Press, 2015).
59. H. Wickham, M. Averick, J. Bryan, W. Chang, L. D. McGowan, R. François, G. Grolemund, A. Hayes, L. Henry, J. Hester, M. Kuhn, T. L. Pedersen, E. Miller, S. M. Bache, K. Müller, J. Ooms, D. Robinson, D. P. Seidel, V. Spinu, K. Takahashi, D. Vaughan, C. Wilke, K. Woo, H. Yutani, Welcome to the Tidyverse. *J. Open Source Softw.* **4**, 1686 (2019).
60. B. Ripley, *tree: Classification and Regression Trees* (R package v. 1.0-40, 2019); https://CRAN.R-project.org/package=tree.
61. S. Garnier, *viridis: Default Color Maps from "Matplotlib"* (R package v. 0.5.1, 2018); https://CRAN.R-project.org/package=viridis.
62. A. Roesch, H. Schmidbauer, *WaveletComp: Computational Wavelet Analysis* (R package v. 1.1, 2018); https://CRAN.R-project.org/package=WaveletComp.
63. D. B. Percival, A. T. Walden, *Wavelet Methods for Time Series Analysis* (Cambridge Univ. Press, 2000); http://ebooks.cambridge.org/ref/id/CBO9780511841040.
64. A. Zeileis, G. Grothendieck, zoo: S3 infrastructure for regular and irregular time series. *J. Stat. Softw.* **14**, 1–27 (2005).
65. J. Bai, P. Perron, Estimating and testing linear models with multiple structural changes. *Econometrica* **66**, 47–78 (1998).
66. D. W. K. Andrews, W. Ploberger, Optimal tests when a nuisance parameter is present only under the alternative. *Econometrica* **62**, 1383–1414 (1994).
67. A. Zeileis, C. Kleiber, W. Krämer, K. Hornik, Testing and dating of structural changes in practice. *Comput. Stat. Data Anal.* **44**, 109–123 (2003).
68. G. Schwarz, Estimating the dimension of a model. *Ann. Stat.* **6**, 461–464 (1978).
69. R. E. Kass, A. E. Raftery, Bayes factors. *J. Am. Stat. Assoc.* **90**, 773–795 (1995).
70. L. Breiman, Ed., *Classification and Regression Trees* (Chapman & Hall [u.a.], 1998).
71. B. Ripley, *Pattern Recognition and Neural Networks* (Cambridge Univ. Press, 1996).
72. W. J. R. M. Priyadarshana, G. Sofronov, Multiple break-points detection in array CGH data via the cross-entropy method. *IEEE/ACM Trans. Comput. Biol. Bioinfirm.* **12**, 487–498 (2015).
73. M. Lavielle, Detection of multiple changes in a sequence of dependent variables. *Stoch. Process. Appl.* **83**, 79–102 (1999).
74. K. Bertin, X. Collilieux, E. Lebarbier, C. Meza, Semi-parametric segmentation of multiple series using a DP-Lasso strategy. *J. Stat. Comput. Simul.* **87**, 1255–1268 (2017).
75. M. Lavielle, Using penalized contrasts for the change-point problem. *Signal Process.* **85**, 1501–1510 (2005).
76. Z. R. Struzik, Wavelet methods in (financial) time-series processing. *Phys. A Stat. Mech. Appl.* **296**, 307–319 (2001).
77. S. Mallat, W. L. Hwang, Singularity detection and processing with wavelets. *IEEE Trans. Inf. Theory* **38**, 617–643 (1992).

Acknowledgments
Funding: Funding for this work was provided by Earth Lab through the University of Colorado Boulder's Grand Challenge Initiative, the USGS North Central Climate Adaptation Science Center, NSF CAREER 1846384, and NSF CNH2-S 2009833. **Author contributions:** V.I., J.K.B., and W.R.T. conceptualized the study and wrote the manuscript. V.I. analyzed the data and designed visualizations. **Competing interests:** The authors declare that they have no competing interests. **Data and materials availability:** Fire data are publicly available through the Monitoring Trends in Burn Severity program (www.mtbs.gov). All data needed to evaluate the conclusions in the paper are present in the paper and/or the Supplementary Materials.

Submitted 31 March 2020
Accepted 24 January 2022
Published 16 March 2022
10.1126/sciadv.abc0020